Case Studies in Thermal Engineering 79 (2026) 107718

Contents lists available at ScienceDirect

Case Studies in Thermal Engineering

journal homepage: www.elsevier.com/locate/csite

Energy and performance improvement of R32-based residential air conditioning using SiO_2 and TiO_2 nanolubricants

M.F. Ismail [a,b,*], M.Z. Sharif [a,b], M.M. Sulhan [a]

[a] Faculty of Mechanical Technology and Engineering, Universiti Teknikal Malaysia Melaka, Hang Tuah Jaya, Durian Tunggal, Melaka, 75150, Malaysia

[b] Fakulti Teknologi Kejuruteraan Mekanikal dan Automotif, Universiti Malaysia Pahang Al-Sultan Abdullah, 26600 Pekan, Pahang, Malaysia

GRAPHICAL ABSTRACT

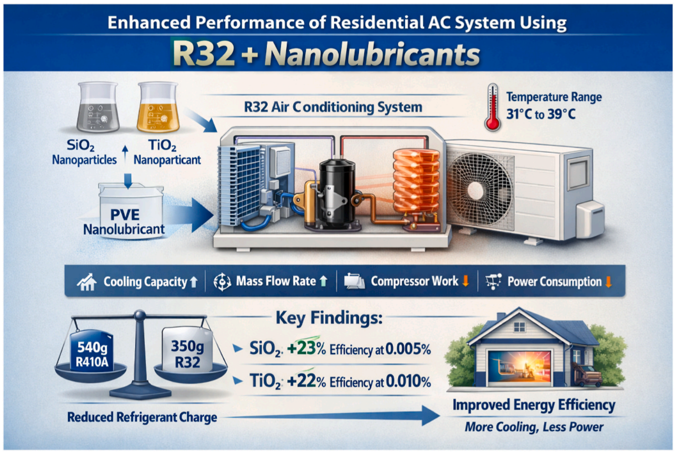

ARTICLE INFO

Keywords:
Nanolubricants
Polyvinyl ether
Refrigeration
PVE

ABSTRACT

This study investigates how SiO_2 and TiO_2 nanoparticle additives improve the performance of a residential air conditioning system operating with R32 refrigerant and PVE lubricant. Improving energy efficiency in home cooling is important because air conditioners consume a large portion of global electricity. Nanolubricants were prepared using a two-step mixing method and tested in a modified R32 system. Testing followed ISO 5151 standard conditions at 35 °C, with performance also evaluated from 31 to 39 °C for comparison. The system performance was evaluated

* Corresponding author.
E-mail addresses: mfarid@utem.edu.my (M.F. Ismail), sharif@utem.edu.my (M.Z. Sharif), sulhan@utem.edu.my (M.M. Sulhan).

https://doi.org/10.1016/j.csite.2026.107718
Received 14 October 2025; Received in revised form 5 January 2026; Accepted 17 January 2026
Available online 20 January 2026

COP
Nanofluid

based on cooling capacity, mass flow rate, compressor work, power consumption, and overall efficiency under steady operating conditions. Results show that replacing the original working fluid with R32 reduces the refrigerant charge from 540 g to 350 g. The use of SiO_2 and TiO_2 nanolubricants reduced compressor work and increased mass flow rate, leading to better heat transfer and cooling output. The highest improvement was recorded at low additive concentrations. SiO_2 at 0.005 percent increased performance by up to 23 percent, while TiO_2 at 0.010 percent increased performance by up to 22 percent. Cooling capacity increased and power consumption decreased compared to pure PVE, enabling the system to deliver more cooling with less electricity. This study provides experimental data for a residential air conditioning system using R32 and PVE based nanolubricants, which has not been reported before. The results show that very small amounts of nanoparticles can improve system efficiency and reduce energy use under real operating conditions. Future work shall also include the study of PVE nanolubricant miscibility and the physical effects of nanoparticles on the compressor electrical motor.

1. Introduction

Residential and commercial sectors consume a significant share of global energy, with electricity demand expected to continue rising due to rapid urbanization and population growth in developing Asian countries due to 40 % growth in the number of households by 2040 [1]. Household appliances such as heaters, refrigerators, freezers, and air conditioners account for approximately 30 % of total electricity consumption [2]. Residential air conditioning (RAC) systems, in particular, have become essential in hot climate regions and are now widely installed in residential buildings. In 2018 alone, more than 97 million RAC units were produced in Asia, making the region the largest global consumer of air conditioning systems [3]. Even modest improvements in RAC efficiency can therefore lead to substantial reductions in overall energy consumption.

In parallel with efficiency improvement, refrigerant selection has undergone major changes due to environmental regulations. Refrigerant development progressed from early natural substances to chlorofluorocarbons, which were later phased out following international agreements. The refrigerant has undergone several transformations, starting with natural substances such as Ethyl-Ether and later Chlorofluorocarbon (CFC), invented in 1928 [4]. As a result of international agreements to phase out CFC in 1987, Hydrochlorofluorocarbon (HCFC) and Hydrofluorocarbon (HFC) were introduced [5]. Hydrofluorocarbons such as R410a subsequently became widely used; however, their high global warming potential has driven the search for alternatives. R32 has emerged as a promising replacement due to its lower global warming potential and favourable thermodynamic properties. For instance, Taira, Haikawa [6] recommend R32 as the best replacement for R410a. Yajima, Kita [7] compare the performance and Total equivalent warming impact (TEWI) of R32 and R410a, revealing that TEWI for R32 decreases by 18 %, and direct impact decreases by 7 %. Recent research has focused on blending R32 with other refrigerants to address some drawbacks, such as flammability levels and high discharge temperature [8]. The mixture aims not only to solve the drawback parameters but also to evaluate the performance of R32 and its ability to increase efficiency Marcucci Pico, da Silva [9].

One approach proposed to further improve RAC energy efficiency is the use of nanoparticle additives dispersed in working fluids [10–14]. Early studies demonstrated that suspending nanoparticles in base fluids can significantly modify thermal and rheological properties. This method was initially investigated by Masuda, Ebata [15] and Choi and Eastman [16] in the hope that the small amount of nanoparticle suspension, namely 'nanofluid' shows a significant impact on the properties of the base fluid. For refrigeration systems, nanoparticle dispersion studies can be categorized into three research avenues [17]. The first approach is nanorefrigerant research, where nanoparticles are suspended onto the pure base refrigerant where the refrigerant is in liquid form under ambient conditions [18]. The second approach is to disperse nanoparticles in the lubricant of a system such compressor in RAC [19]. Commonly called a nanolubricants, this method appeared preferable among researchers as lubricants usually have high boiling temperatures, and dispersion processes can be done at room temperature. The third method is the dispersion of nanoparticles in pure lubricant, then applied in refrigerant-based equipment to enhance the performance of the refrigeration systems in the two-phase flow phenomena [20]. Boiling and condensation are this research strategy's most popular performance examination [21,22]. Meanwhile, a performance study on the vapor compression refrigeration (VCR) cycle with nanolubricants-refrigerant mixture widened the research area and positively impacted the energy efficiency research path [23].

A recent study investigated the performance of nanolubricants on the VCR system when operating with R32 [9]. The research was conducted using diamond nanoparticles dispersed in polyol ester (POE) oil. Carbon nanotubes (CNT) have also been investigated for refrigeration applications due to their very high thermal conductivity and strong ability to enhance heat transfer [24]. Several reports show that CNT based nanolubricants can reduce compressor work and increase cooling performance, making them a potential candidate for comparison with SiO_2 and TiO_2 in future studies. The polyvinyl ether (PVE) is a new alternative lubricant for HFC refrigerant i.e., R32. PVE is more soluble with R32 than POE [25] and has several additional advantages. Firstly, PVE does not hydrolyse, making using a hydrolysis filter dryer unnecessary and preventing capillary tube blockages. Secondly, PVE has a flexible polymer property, allowing for optimal modification of its viscosity and miscibility. Finally, PVE is effective with extreme pressure agents [26]. As a result of these benefits, studies have been conducted on PVE's properties to assess its performance as a lubricant in a VCR system [27–29]. Additionally, recent research has focused on the physical properties of PVE when mixed with nanoparticles and refrigerant [30]. Despite the extensive research on the impact of nanoparticles on various refrigerants [31], there have been no studies examining the effect of nanoparticles on the performance of R32/PVE in RAC systems.

Table 1
Properties of PVE base lubricant [26] and R32 [51].

Property	PVE FVC68D	R32
Dynamic Viscosity, [mm2/s @ 40 °C]	68.1	
Dynamic Viscosity, [mm2/s @ 100 °C]	8.04	
Viscosity index	84	
Pour Point, [°C]	−37.5	
Flash point, [°C]	204	
Density, [kg/m3 @ 15 °C]	936.9	
Boiling point [°C]		−51.65
Critical condition:		
- pressure [MPa]		5.78
- temperature [°C]		78.1
Environmental impact (ODP/GWP)		0/675
ASHRAE safety code		A2L

Table 2
Properties of SiO_2 and TiO_2 nanoparticles at room temperature [52,53].

Property	Nanoparticles	
	SiO_2	TiO_2
Density, ρ [kg/m3]	2220	4230
Thermal conductivity, k [W/mK]	4	8.4
Molecular mass, M [g/mol]	60.08	79.87
Average particle diameter, d_p [nm]	15	30–50
Specific surface area [m2/g]	250	–
Specific heat, cp [J/kgK]	745	692
CAS number	14808-60-7	13463-67-7

To address this gap, the present study experimentally investigates the performance of a residential air conditioning system operating with R32 refrigerant and polyvinyl ether based nanolubricants containing SiO_2 and TiO_2 nanoparticles. The study includes the production of nanolubricants using a two-step method, followed by stability assessment and characterization through a high-resolution transmission electron microscope. The RAC test rig was installed and commissioned following standard procedures, and data were collected under steady-state conditions. The experimental analysis involved evaluating the VCR cycle's performance using pressure and temperature data, while flow meters and power analysers collected additional data to determine the cooling capacity, total power consumption, and energy efficiency ratio of the RAC system. To ensure the reliability of the experimental results, the study also includes an uncertainty analysis of the measurement data. The findings of this study provide valuable insights into the potential benefits of using nanolubricants in RAC systems and add to the existing knowledge in the field of heat engineering.

2. Methodology

2.1. Nanolubricants preparation and stability evaluation

R32 refrigerant was used as the working fluid because of its widespread application in residential air conditioning systems. The refrigerant was supplied in a certified 3 kg non recyclable cylinder. The compressor lubricant was polyvinyl ether oil, PVE FVC68D, supplied by Idemitsu Kosan Co., Ltd. The thermophysical properties of R32 and PVE are listed in Table 1. SiO_2 nanoparticles were supplied by DKNANO, Beijing Deke Daojin Science and Technology Co., Ltd., and TiO_2 nanoparticles by HWNANO, Hongwu International Group Ltd. Both nanoparticles had a declared purity of 99.9 percent, with mean particle sizes of 15 nm for SiO_2 and 30 nm for TiO_2. Unused nanoparticles were stored in a dry cabinet under controlled temperature and humidity to minimize moisture absorption. No pre-treatment or heat treatment was applied. The detailed properties of the nanoparticles are summarized in Table 2.

Nanolubricants were prepared using the two step dispersion method recommended by Nabil, Azmi [32]. SiO_2 PVE nanolubricants were prepared at concentrations between 0.003 and 0.010 vol percent, while TiO_2 PVE nanolubricants ranged from 0.005 to 0.020 vol percent. Preliminary testing showed a clear degradation in RAC performance when the concentration exceeded 0.010 vol percent. Similar concentration ranges have been reported in earlier studies [33–35]. Therefore, the present study focused on the lowest practical concentrations to ensure stable operation. The required nanoparticle mass was measured using a high precision digital balance with ±0.0001 accuracy. The volume concentration was calculated using Eq. (1) [36,37]:

$$\phi = \frac{\frac{m_n}{\rho_n}}{\frac{m_n}{\rho_n} + \frac{m_l}{\rho_l}} \times 100\% \tag{1}$$

where ϕ is the concentration in volume percent, m_l and m_n are the masses of PVE lubricant and nanoparticle, respectively, while ρ_l and ρ_n are the density of PVE lubricant and nanoparticle, respectively. At least 320 ml of PVE oil was used for each formulation.

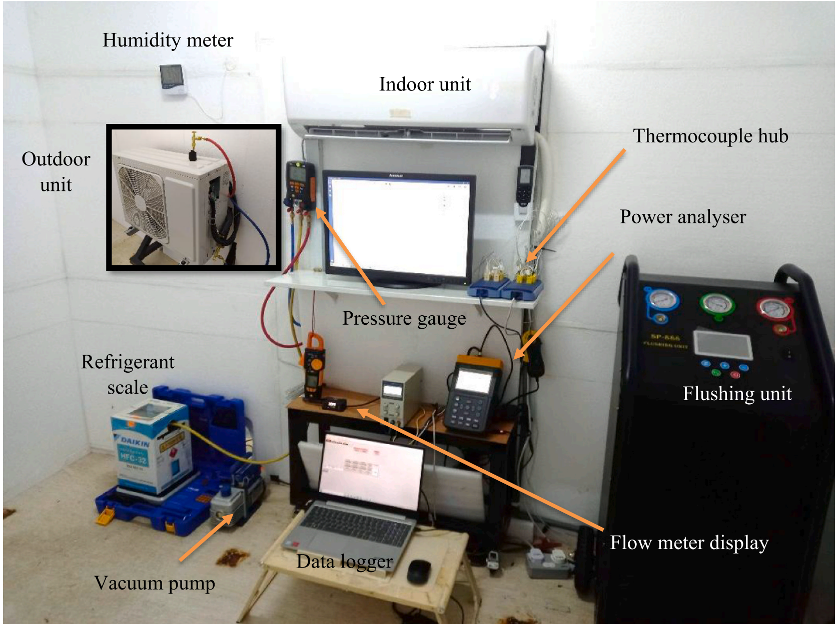

(a) Test setup for indoor and outdoor

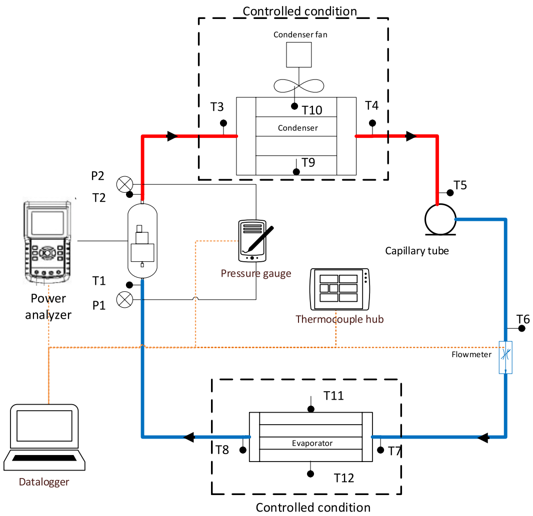

(b) Schematic diagram

Fig. 1. RAC Test rig.

Nanoparticles were first dispersed using magnetic stirring for 0.5 h, followed by ultrasonication in a Fisherbrand 15051 ultrasonic bath for 7 h for both SiO_2 PVE and TiO_2 PVE nanolubricants [38]. The ultrasonic bath operated at a mean power of 80 W and a frequency of 37 kHz. For visual sedimentation observation, 15 ml of each nanolubricant was transferred into a test tube, while 5 ml was reserved for zeta potential analysis [39]. Microstructural characterization was conducted using a TECNAI G2 F20 X Twin high resolution transmission electron microscope.

2.2. RAC test-rig description

A customized split type residential air conditioning hanger was used to assemble the experimental rig, consisting of an indoor and an outdoor unit. The system had a rated cooling capacity of 9000 Btu h^{-1} and was installed in accordance with the manufacturer service manual provided by Gree Electric Appliances Inc. of Zhuhai. The unit employed a rolling piston rotary compressor originally designed for R410a operation. All installation work, including electrical wiring, refrigerant piping, insulation, and condensate

Table 3
Summary of materials and equipment for the experiment

Materials/ Equipment	Description
Indoor unit	Consist of evaporator, blower fan, and electronic control board
Outdoor unit	Consist of rolling piston rotary compressor, condenser, condenser fan, capillary tube, discharge and suction valve, and flow meter sensor head
Thermocouple hub	Pico Datalogger: Each unit contains 8 channels of thermocouples, connecting to data logger by USB interface.
Pressure gauge	Testo 2-way manifold to measure discharge and suction pressure. Data collection via Bluetooth and apps
Flow meter	Consist of sensor head, controller and display, and clamp to measure liquid refrigerant
Power analyser	3-phase power analyser from Prova (6830A) used to measure power consumption. Connected to datalogger by RS232C to USB interface
Refrigerant scale	Digital weigh scale with automatic controller to charge refrigerant into RAC system accurately
Flushing unit	3 in 1 refrigerant recovery, flushing and charging. Used to recover refrigerant, flushing, and collecting lubricant
Vacuum pump	Single stage vacuum pump (Value model VE115N) 2CFM. Used to evacuate air from the RAC system up to 150 μm
Humidity meter	To measure instantaneous humidity in the indoor and outdoor area
Datalogger	Consist of a personal computer connected to Pico datalogger (16 channel), Power analyser, and additional data display.

Table 4
Test rig instrumentation ranges and uncertainty

Measured data	Model	Measuring range	Uncertainty
Pressure	Testo 550 digital pressure gauge	−0.1 to 6 MPa	±0.5 %
Temperature	RS PRO K-type 0.6 mm	−50 to 250 °C	±0.1 °C
Power consumption	Prova 6830A power & harmonics	1–10 kW	±0.01 kW
Flowrate	Keyence FD-XS8	0 to 3000	±2.9 mL/min

Table 5
Air temperature during RAC operation according to ISO5151:2010 [54].

Parameter	T1 – Standard rating temperature (°C)	
Temperature of air entering indoor	Dry bulb	27
	Wet bulb	19
Temperature of air entering outdoor	Dry bulb	35
	Wet bulb	24

drainage, was carried out using appropriate tools and personal protective equipment. The indoor and outdoor units were connected by copper pipes with diameters of 6.35 mm on the liquid line and 9.52 mm on the gas line. The indoor airflow rate was 580 $m^3 h^{-1}$, with a nominal power input of 0.819 kW and a current of 3.22 A.

The test rig was installed inside a thermal control room designed in accordance with ISO 5151:2010. The facility comprised separate indoor and outdoor chambers. Fig. 1(a) shows the experimental arrangement from the indoor side, with the outdoor unit positioned across a partition wall. A summary of the main apparatus and equipment is provided in Table 3. Fig. 1(b) presents the schematic diagram of the system, showing sensor locations and connections to the data acquisition system. Instrumentation ranges and measurement uncertainties are listed in Table 4.

2.3. Apparatus commissioning

After installation, the system was inspected and tested both at component level and as an integrated unit. Electrical connections were carefully checked to prevent current leakage. A leak test was performed on the entire refrigerant circuit, including all copper joints and manifold connections. The system was then evacuated using a vacuum pump to remove moisture and non-condensable gases. A 12 h vacuum holding period was applied to confirm leak free conditions. The system was subsequently charged with 225 g of R32 refrigerant. All experiments were conducted under T1 standard indoor and outdoor conditions, as listed in Table 5.

All thermocouples were calibrated against a mercury thermometer that had been previously calibrated by Redhwan, Azmi [40] and Taib, Aziz [41]. Calibration was carried out at freezing, ambient, and boiling temperature points prior to installation. The pressure gauges, power analyzer, and flow meter were calibrated by a certified laboratory, and their respective uncertainties were included in the data analysis.

2.4. Experimental procedure

In this study, the R32 refrigerant was utilized as a drop-in replacement for the R410a RAC system. Prior to conducting the experiment with nanoparticles additives, the optimum refrigerant charge was determined. The RAC system was charged with R32 refrigerant in intervals of 25 g, ranging between 225 g and 375 g. The T1 condition was maintained, and the RAC system was operated

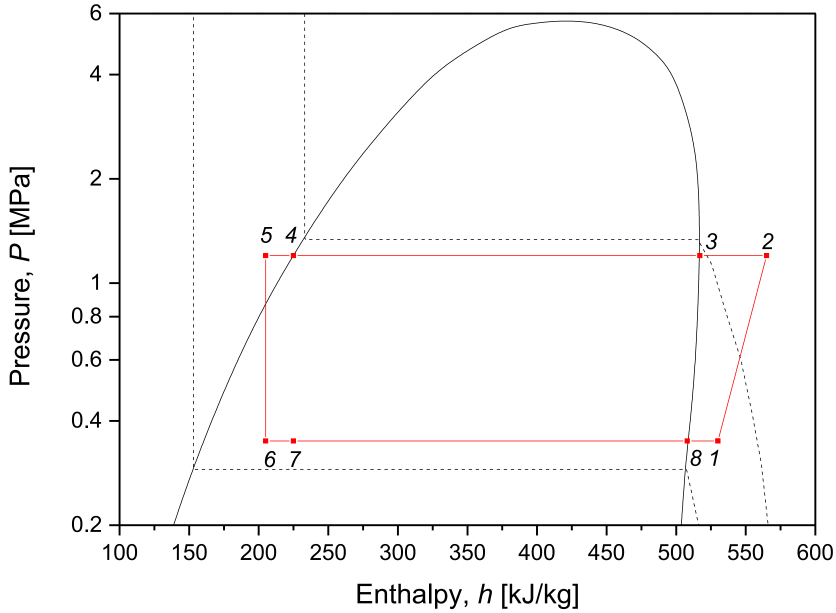

Fig. 2. P-h diagram of present VCR system cycle for R32 refrigerant.

continuously for 1 h until it reached a steady-state condition. The test data was collected every 2 min during the first hour to confirm the steady-state condition. Once achieved, data collection was carried out for an additional 30 min, which was repeated three times. The average value for each parameter was determined and used as the final experimental result.

Following the determination of the optimum refrigerant charge, the experiment examining the effect of nanoparticles additives on the RAC was carried out. The indoor area was maintained at the T1 condition, while the outdoor temperature was varied between 31 and 39 °C with an increment of 39 °C. The same method was employed for data collection. Upon completion of data collection for each sample, the refrigerant was recovered, and the lubricant was collected using a flushing machine. To avoid cross contamination between successive tests, the flushing process was continued until no visible residue of the previous lubricant remained in the system. The flushing unit utilized in the process consisted of a compressor, an external refrigerant tank, a cooling system, a pressure gauge, and a control system. The flushing unit was connected to the RAC system via two manifolds, namely the suction and discharge lines. The compressor pumped the refrigerant from the external tank to the RAC piping through the discharge line. The connection in the suction line recovered the refrigerant back to the flushing unit. A filter within the flushing unit separated the oil and refrigerant, with the process continuing for 10 min before the flushing process switched in the reverse direction. The flushing process was repeated multiple times until the volume of lubricant collected was equivalent to the filled volume before each experiment. Fresh nanolubricant was prepared for each concentration and test condition, and only newly prepared samples were charged into the compressor. This study evaluates nanolubricant performance using a complete residential air conditioning system operated under ISO 5151 conditions. Performance was assessed through direct measurements of cooling capacity, mass flow rate, compressor work, power consumption, COP, and EER. The system was tested using a drop-in replacement of R32 and PVE lubricant without altering the original hardware configuration. Very low nanoparticle concentrations were selected to ensure stable operation while maintaining measurable performance enhancement. Nanolubricant stability was verified prior to system testing using visual observation, zeta potential analysis, and HRTEM characterization, ensuring consistency during operation.

2.5. Experimental analysis

The experimental analysis in the current study is divided into two. The first analysis only focuses on the investigation of the performance of the refrigeration cycle. The pressure and temperature data were collected to calculate the crucial parameter including enthalpy for compressor suction (h1), enthalpy for compressor discharge (h2), and enthalpy for evaporator inlet (h6). The refrigerant effect (qin), compressor work (Win), and coefficient of performance (COP) were calculated to evaluate the performance of the VCR cycle.

The second analysis of the experiment covers the investigation of the performance of the RAC system. Additional to the data from the first analysis, data from the flow meter and power analyser was also collected to calculate the cooling capacity ($\dot{q}_c$), total power consumption (Psys), and energy efficiency ratio (EER) for the RAC system. The second stage of the experiment uses both analysis methods in determining the effect of nanoparticles additive to the performance of the VCR cycle and the RAC system.

A P-h diagram for R32 refrigerant as in Fig. 2 was used to analyse the experimental data. The calculations and analysis in this paper assume the ideal condition of the VCR cycle. The cooling effect in the evaporator is evaluated by the evaporator ability to absorb heat

Table 6
Percentage of relative standard error for the experimental performance parameters

Ambient temperature	Percentage relative standard error, RSE (%)					
	q_{in}	Win	COP	$\dot{q}_c$	Psys	EER
31	0.37	0.74	0.70	3.71	0.34	3.73
33	0.32	0.24	0.39	4.39	0.11	4.19
35	0.26	0.32	0.41	4.75	0.38	4.27
37	0.06	1.29	1.29	4.76	0.21	4.74
39	0.14	1.06	0.99	4.41	0.28	4.11

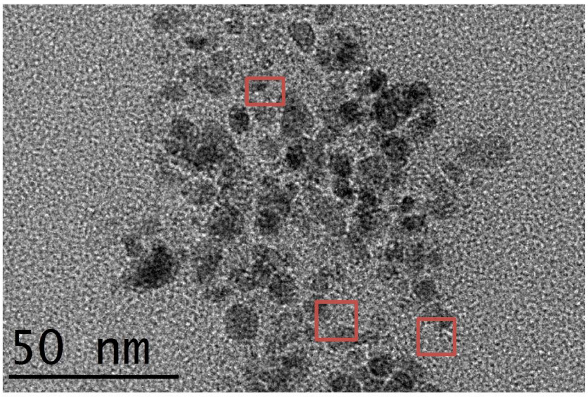

(a) SiO_2/PVE

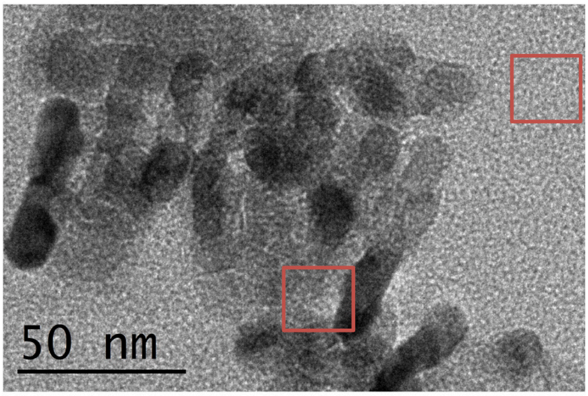

(b) TiO_2/PVE

Fig. 3. HRTEM image of nanolubricants.

load and the cooling capacity as determined in Eqs. (2) and (3) respectively

$$q_{in=h_1-h_6} \tag{2}$$

$$\dot{q}_{c=\dot{m}(h_6)} \tag{3}$$

where $\dot{m}$ is the refrigerant mass flowrate (kg/s) at the liquid line. The effect of the variable on the compressor is evaluated by the compressor work in Eq. (4)

$$w_{in=h_2-h_1} \tag{4}$$

The efficiency of the VCR cycle and RAC system was determined by the COP and EER in Eqs. (5) and (6), respectively

$$COP = \frac{q_{in}}{w_{in}} \tag{5}$$

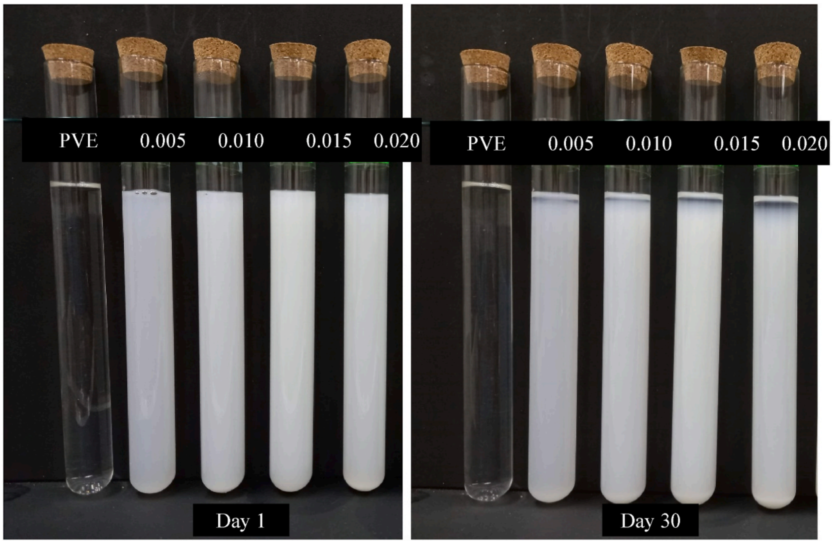

(a) TiO2/PVE

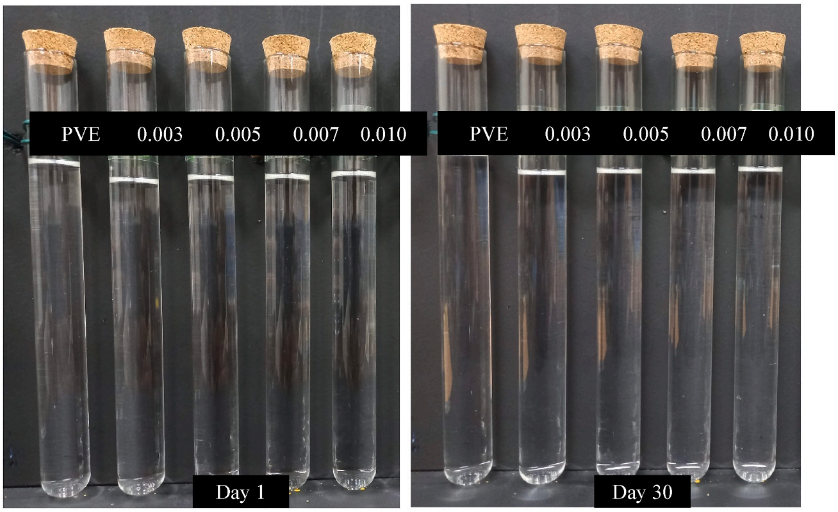

(b) SiO2/PVE

Fig. 4. Nanolubricants stability observation on the 1st and 30th day after preparation.

$$EER = \frac{\dot{q}_c}{P_{sys}} \tag{6}$$

In analysing the performance of VCR and RAC in ideal condition, the following assumptions are considered: (i) the pressure difference between discharge and condensation can be ignored, (ii) the pressure difference between evaporator inlet and outlet can be ignored, (iii) isentropic expansion in the capillary tube makes the enthalpy of condensation is same as evaporator inlet (h5 = h6), (iv) cooling capacity of heat removal from the indoor area is same as the cooling capacity of heat absorbed by the refrigerant, (v) the heat transfer on connection pipes to the environment or insulator can be ignored.

2.6. Uncertainty analysis

Measurement uncertainty was evaluated using the percent relative standard error, RSE, following the methodology reported by Sharif, Azmi [42] and Redhwan, Azmi [43]. The consistency of the measured data was quantified using Eq. (7), with the standard error Seer calculated using Eq. (8). Here, X denotes the sample mean, σ the standard deviation, and n the number of samples. Each experiment was repeated three times, and the average RSE was reported for each parameter. The uncertainties associated with all

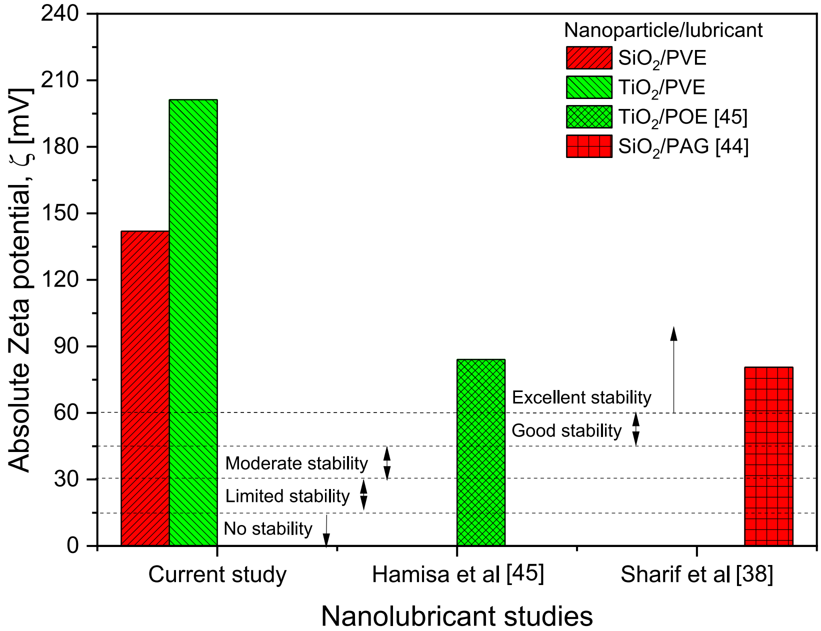

Fig. 5. Zeta potential measurement of nanolubricants in comparison with literature.

measured variables are listed in Table 6. The maximum RSE was 4.76 percent, which is within acceptable experimental limits.

$$RSE\ (\%) = \frac{S_{eer}}{X} \times 100 \tag{7}$$

$$S_{eer} = \frac{\sigma}{\sqrt{n}} \tag{8}$$

3. Results and discussion

3.1. Stability of nanolubricants

Nanolubricants stability is essential to be evaluated before being applied in the actual RAC system. Even though the nanolubricants in the VCR cycle continuously moves in the system cycle, there is a period when the system does not in operation. The nanolubricants will be in stagnant condition for a long time. The nanolubricants in stagnant conditions tends to form larger aggregates and settle down due to their weight and gravitational force. Therefore, stability evaluation in this paper was conducted on stationary nanolubricants by visual sedimentation observation. Zeta potential analysis was conducted to evaluate the stability quantitatively. Additionally, an HRTEM examination was carried out on the nanolubricants to evaluate their dispersion distribution and confirm the size of nanoparticles. Fig. 3 depicted the results of HRTEM for both types of nanolubricants. The nanoparticle was evenly distributed in the lubricant with some agglomeration occurring. The size of SiO_2 nanoparticles was confirmed in the range of 15 nm while TiO_2 nanoparticles are between 30 and 50 nm.

3.2. Visual sedimentation observation

The stability evaluation by visual observation was conducted for 30 days. Fig. 4 (a) shows the comparison of TiO_2/PVE nanolubricants between the first and the 30th day after preparation. The pure PVE lubricant was placed together as a reference. After the 30th day, all TiO_2/PVE nanolubricants do not exhibit many changes in appearance. The only difference observed is the clear layer of oil appeared on the top of the lubricant. The layer was very small for nanolubricants with 0.005 vol% concentration. However, by the increment of concentration, the layer appeared to be wider. The SiO_2/PVE nanolubricants in Fig. 4 (b) have no colour and appeared slightly different with the pure PVE lubricant. After 30 days, there are 10 mm clear layer appeared on the top side of the nanolubricants. The small clear layer indicates some agglomeration has started being developed in the nanolubricants. The nanoparticles clump has been falling off to the lower side of the test tube due to the gravitational effect on its weight. Even though TiO_2/PVE and SiO_2/PVE nanolubricants show some changes, the overall observation indicates that both types of nanolubricants have good stability. The visual observation of nanolubricants stability shall be evaluated quantitatively to confirm the results from visual observation. Zeta potential is the best method to confirm the stability of nanolubricants.

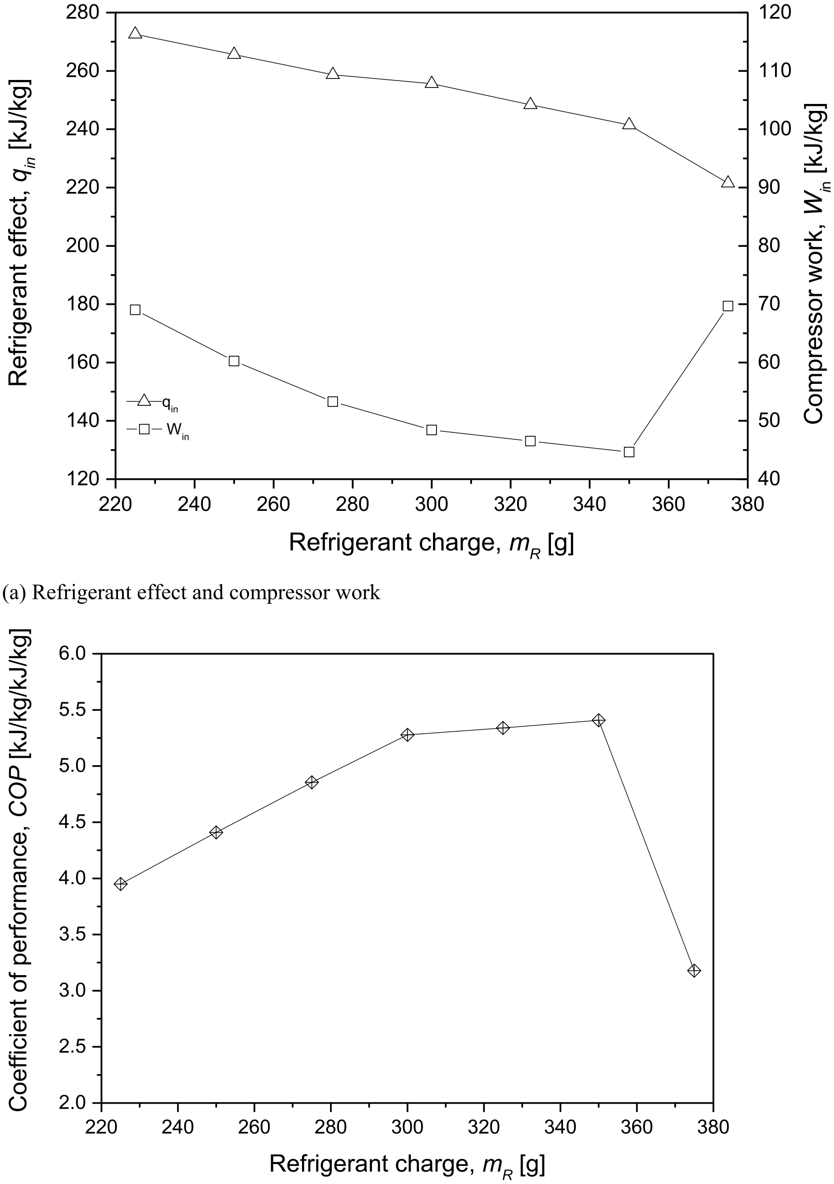

(a) Refrigerant effect and compressor work

(b) COP

Fig. 6. R32/PVE VCR system performance comparison at different refrigerant charge.

3.3. Zeta potential analysis

Zeta potential quantifies the difference in potential between the PVE lubricant-charged ions and the oppositely charged ions on nanoparticle surface. The greater the size of the potential, the greater the electrostatic repulsion and hence created better stability. The current study's zeta potential measurements were compared with data from the literature as shown in Fig. 5 [44,45]. According to Ghadimi, Saidur [46], the nanofluid that has greater than ±60 mV zeta potential is considered to have excellent stability. The results show that both SiO_2/PVE and TiO_2/PVE nanolubricants have excellent stability. Similar results show TiO_2 nanoparticles in POE and SiO_2 nanoparticles in poly alkyl glycol (PAG) oil also have excellent stability. The only difference is the current study provides a higher zeta potential value compared to others from the literature.

The zeta potential measurement results had confirmed the visual observation stability in Fig. 4 quantitatively. Both SiO_2/PVE and TiO_2/PVE nanolubricants have excellent stability without any sedimentation appearing for up to 30 days. The results indicate that both types of nanolubricants are suitable for application in the RAC system because the nanolubricants remains in excellent stability for more than 30 days. No sedimentation will occur if the RAC is left unoperated within the first 30 days.

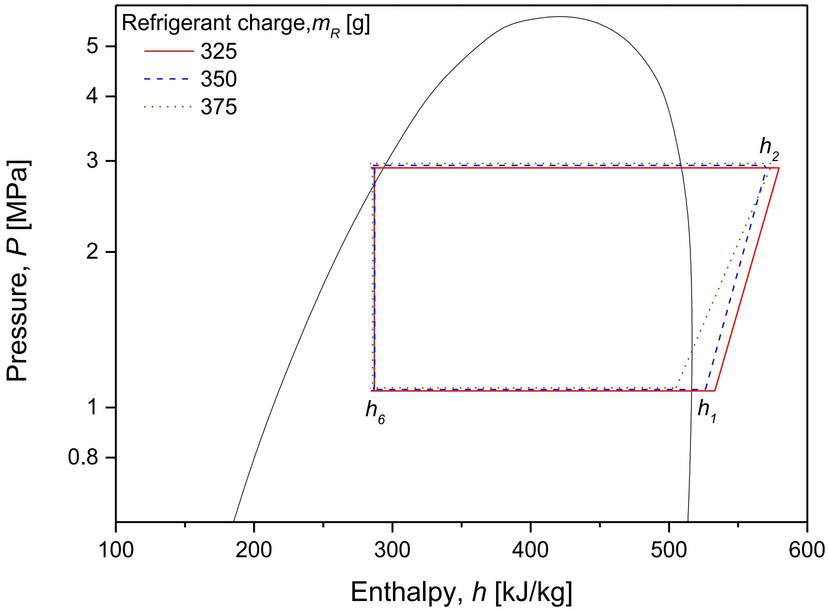

Fig. 7. P-h diagram plot for three different refrigerant charge.

3.4. Performance of R32/PVE

The RAC system used in this paper was originally manufactured for refrigerant R410a. Since the R32 was used as a drop-in refrigerant in the RAC system, the optimum charge for R32 shall be determined first before further investigation on the system performance. Fig. 6 (a) represents the refrigerant effect and compressor work of R32/PVE for a refrigerant charge between 225 and 375 g. The trend line indicates that the refrigerant effect decreases by the increase of charge. The decrement is at a constant rate for a refrigerant charge between 225 and 350 g. At 375 g, the refrigerant effect decreases at a higher rate make the refrigerant effect value drop to 239 kJ/kg drastically. For compressor work, the decrement trend appeared when the refrigerant charge increase. However, the compressor work value suddenly increases to the highest point when the system was charged to 375 g. Further analysis on the VCR cycle is the COP presented in Fig. 6 (b). The COP of the system increased for the charge at 250 g–350 g. The COP achieves its optimum at 350 g before drastically dropping to the lowest value at 375 g.

All the three parameters in Fig. 6 show that there are steady changes when the system was charged between 225 g and 350 g. A strange trend appeared when the charge is higher than 350 g. The 350 g refrigerant charge is selected as the optimum charge for R32 due to the maximum value of COP. The trend line indicates that the RAC system was in overcharged condition when 375 g R32 refrigerant was charged into the system. At this point, the refrigerant effect drastically decreases, and the compressor work jumped to the highest value. Ultimately, the COP reduced to the lowest level compared to other refrigerant charges.

The undercharge, optimum, and overcharge condition is easier to explain by using the P-h diagram as shown in Fig. 7. The VCR cycle lines displayed in this figure represent the ideal refrigeration cycle for 325, 350, 375 g. The lines were plotted using the actual experimental data for the respective refrigerant charge. The three conditions can be differentiated by focussing on h1, h2, and h6. The 325 g that represents undercharge condition has the highest refrigerant effect where the superheat temperature is the highest compared to others. The refrigerant enters the compressor at a high temperature because the amount of refrigerant is not enough. The compressor is starved of refrigerant to compress makes the discharge temperature increase. At 350 g, the amount of refrigerant is just enough to the need of compressor without starving of refrigerant. The compression slope slightly increases makes discharge temperature reduced. Different conditions happened for the 375 g charge where the refrigerant is not fully saturated gas. Some liquid refrigerant entering compressor makes it difficult for the compressor to compress the refrigerant. Consequently, the heat produced from the compression process increases. Thus, discharge temperature and pressure increase. The compressor work increases due to the increment in discharge temperature. This condition increases the COP of the VCR cycle. Additionally, the overcharged system reduced the refrigerant effect that makes worsened the COP value. Therefore, the best refrigerant charge for the current study was decided at 350 g. The RAC system was charged with 350 g R32 refrigerant for the second stage investigation on the nanolubricants effect on the system.

3.5. Nanoparticle effect on ideal VCR performance

This section discusses the effects of nanoparticle additive on the performance parameters of the VCR cycle: refrigerant effect, mass flow rate, and compressor work. Fig. 8 represents the comparison of SiO_2 and TiO_2 additives into the PVE lubricant to the refrigerant

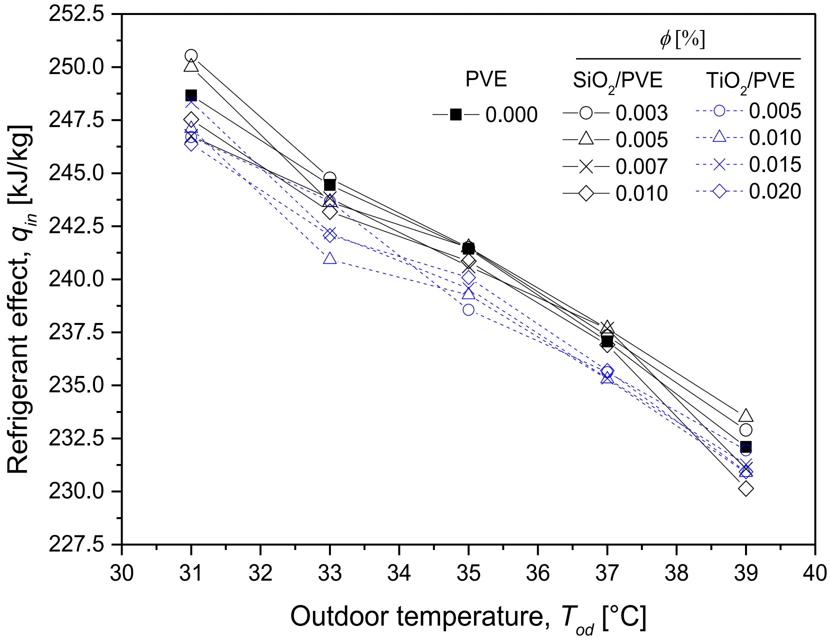

(a) Refrigerant effect

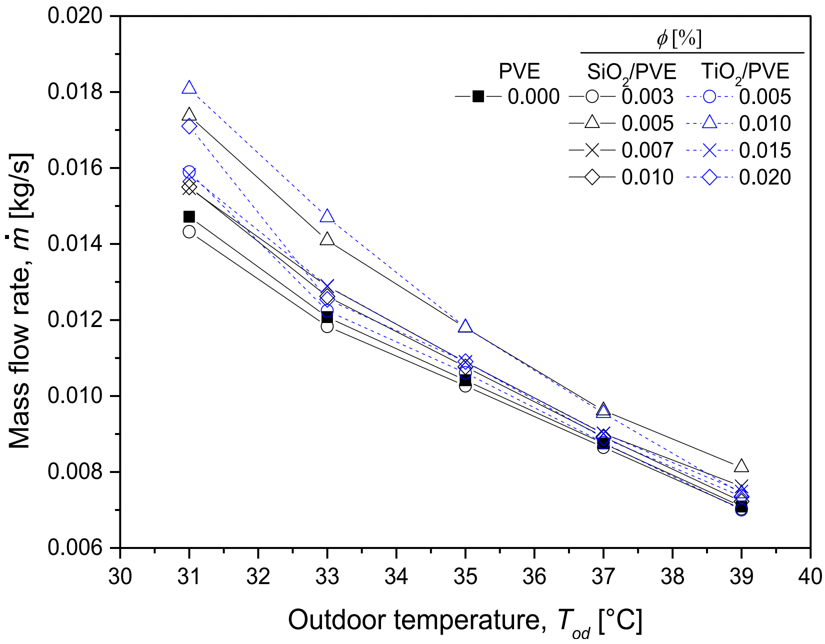

(b) Mass flow rate

Fig. 8. Comparison of refrigerant effect and mass flow rate at different outdoor temperature and concentrations.

effects. The refrigerant effects of pure PVE were also presented for comparison. The overall view showed that the refrigerant effect decreased with the increase in outdoor temperature. The decrement for all samples was shown almost a similar trend. For each outdoor temperature point, almost all nanolubricants showed a lower refrigerant effect than that for the pure PVE lubricant except for SiO_2/PVE at 0.005 % and 0.010 % concentration. The TiO_2/PVE nanolubricants showed a lower refrigerant effect than SiO_2/PVE nanolubricants despite outdoor temperature differences. The most significant decrement happened at 33 °C outdoor temperature.

Based on the findings of other researchers in the literature, the presence of nanoparticles in the evaporator increased the refrigerant effects due to an increment in thermal conductivity [44,47]. Those researchers stated that the heat transfer capability of the evaporator

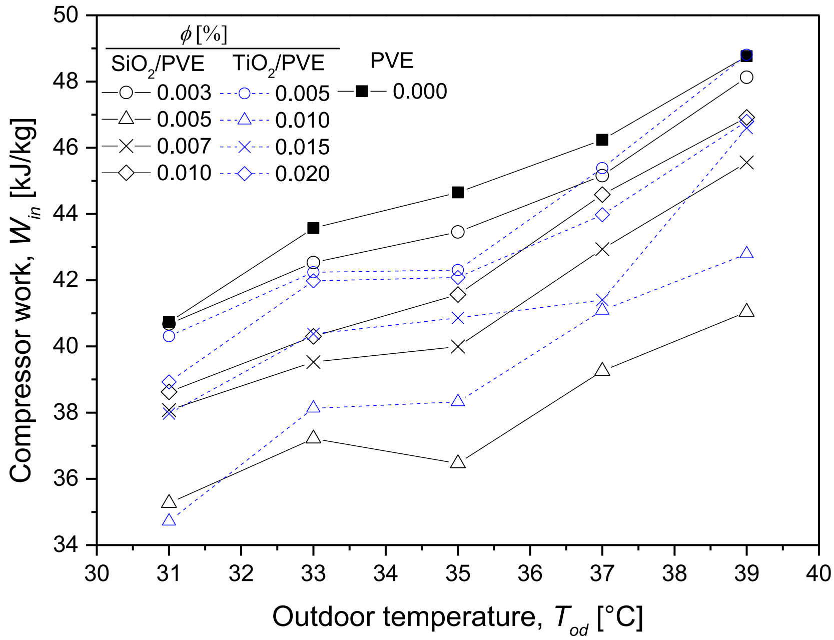

Fig. 9. Comparison of compressor work for nanolubricants at different outdoor temperatures and concentrations.

increased by the increment of nanoparticle concentration. However, the result of refrigerant effects in the current study shows that the refrigerant effect for nanolubricants decreased with the increase volume concentration. The reason of this unsimilar trend mainly contributed by different approach of data collection between the current study and the approach used by Harichandran, Paulraj [48] and Sharif, Azmi [44]. In the current study, only two parameters were varied, (volume concentration, outdoor temperature) while the RAC system used in this study was allowed to regulate other parameters to reach the optimum conditions as explained in the previous chapter. Therefore, the refrigerant effect results in Fig. 8 were influenced by other uncontrolled parameters such as the variation of refrigerant mass flow rates. To understand this situation, it is good to analyse the result of mass flow rates for the same nanolubricants. The results of the mass flow rate for SiO_2/PVE and TiO_2/PVE nanolubricants are shown in Fig. 9.

In Fig. 9, the mass flow rate was measured between outdoor temperature of 31 and 39 °C. The value of mass flow rate for pure PVE lubricant fell between 0.007 and 0.015 kg/s at the measured temperatures. The mass flow rate results for SiO_2/PVE and TiO_2/PVE nanolubricants were plotted together by using a different notation for comparison purposes. Nanolubricants showed that the mass flow rate fell between 0.007 and 0.019 kg/s for the same temperature range. The mass flow rate of nanolubricants showed decreasing trends with the increase in outdoor temperatures from 31 to 39 °C. At the same time, the mass flow rate of nanolubricants increased compared to that of the pure PVE lubricant except for SiO_2/PVE nanolubricants at 0.003 % concentration. The mass flow rate for the lowest concentration for both nanolubricants showed the lowest value of mass flow rate compared to that of other concentration. It was also shown that the second lowest concentration resulted highest mass flow rate than that of other concentration except for TiO_2/PVE at 0.020 %. The result of mass flow rate variation in this figure shows that the mass flow rate was influenced by volume concentration. Additionally, when this result was compared to refrigerant effect in Fig. 8 (b), there is a significant relationship between those parameters. When the mass flow rate increase, the refrigerant effect decreases and vice versa. Therefore, the results of mass flow rate had proved that the refrigerant effect was influenced by the variation of mass flow rate. Comparing the mass flow rate between the different types of nanolubricants, sometimes the TiO_2/PVE nanolubricants showed a higher value than that of SiO_2/PVE nanolubricants but it was in the other way at another concentration. Overall observation shown that nanolubricants resulted higher value of mass flow rate than that of pure PVE. The difference in mass flow rate behavior between SiO_2 and TiO_2 nanolubricants at low concentrations is attributed to their distinct physical properties and interaction with the base lubricant. SiO_2 nanoparticles have smaller size and higher specific surface area, which can increase lubricant viscosity at very low concentrations and slightly restrict refrigerant circulation. In contrast, TiO_2 nanoparticles have higher density and larger particle size, promoting more effective load bearing and friction reduction in the compressor without significantly increasing viscosity. As a result, TiO_2 nanolubricants do not exhibit the initial reduction in mass flow rate observed for SiO_2 at low concentrations.

At the evaporator, heat transfer happened between refrigerant and the surrounding air where the refrigerant exchange heat with air to provide cooling condition to the surrounding. The refrigerant that entered the evaporator required time to absorb heat from the surroundings to evaporate from liquid to gas. A higher mass flow rate increased the refrigerant speed, thus reducing the time for the refrigerant to absorb heat from the evaporator coil. Consequently, less heat absorption process was conducted by the refrigerant, while some refrigerants do not fully evaporate before returning to the compressor. The refrigerant effect was influenced by both the thermal conductivity and by the mass flow rate. The increment and decrement of both parameters determined the changes in heat transfer rate

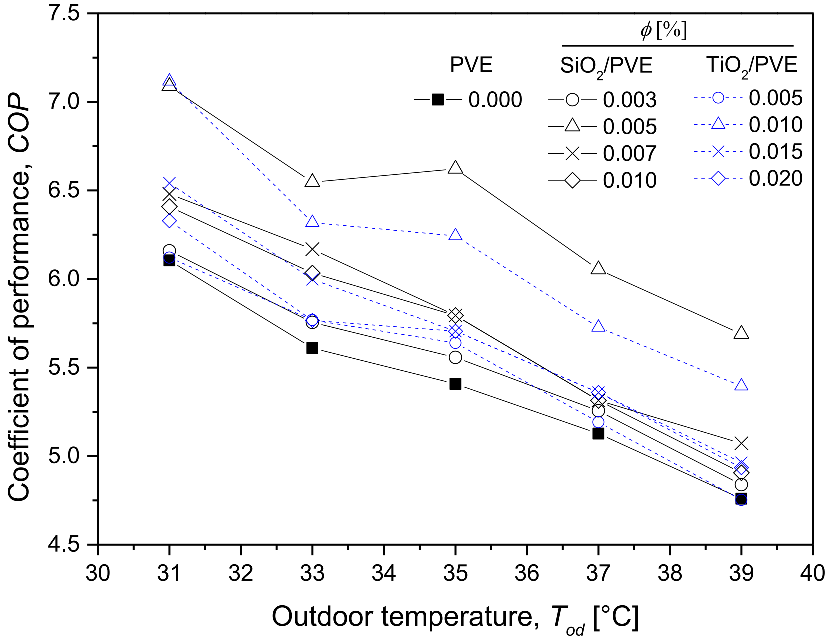

Fig. 10. COP comparison of nanolubricants at different outdoor temperatures and concentrations.

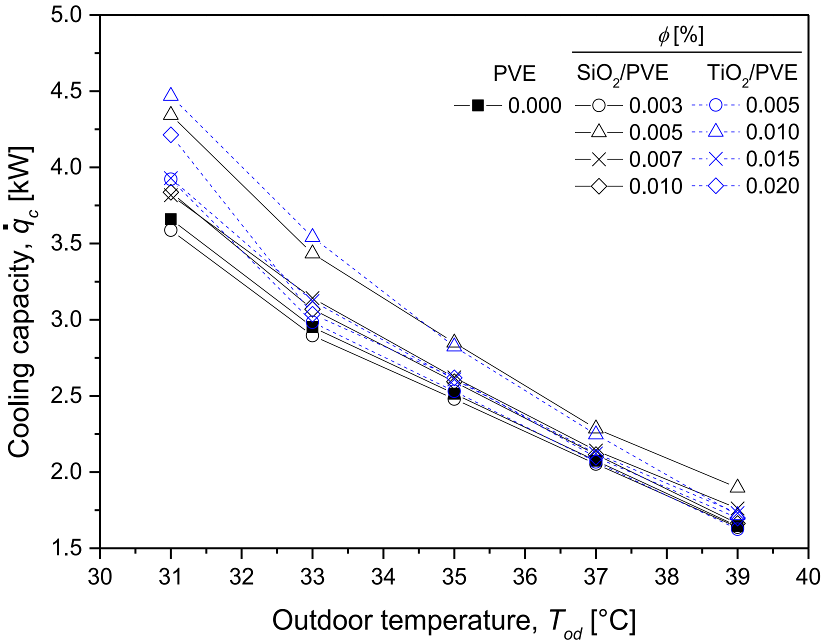

Fig. 11. Comparison of cooling capacity for nanolubricants at different outdoor temperatures and concentrations.

in the evaporator, thus affecting the overall refrigerant effects. The reduction in refrigerant effect observed for most nanolubricant samples is primarily related to the increase in refrigerant mass flow rate. The presence of nanoparticles improves lubrication inside the compressor, allowing smoother compression and higher refrigerant circulation. The results of the refrigerant effect and mass flow rates shown in Figs. 8 and 9 demonstrate that the refrigerant effect was predominantly influenced more by the mass flow rate than by the thermal conductivity.

Another parameter that could be analysed to support the above argument is the compressor work. The changes in mass flow rate were partly affected by the compressor as the compressor was the only component responsible for the compression and the movement of the refrigerant. Therefore, the changes in compressor work might also become an explanation of the mass flow rate as well as the

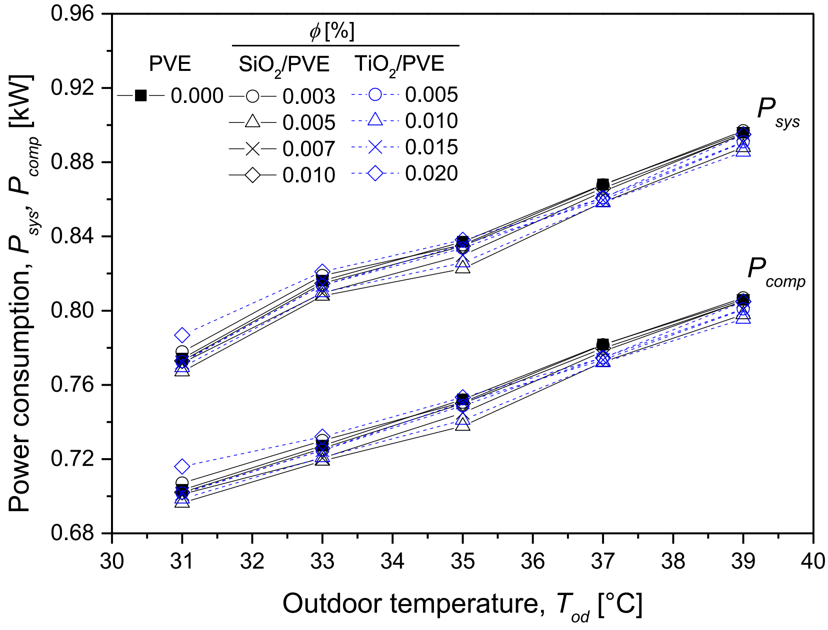

Fig. 12. Comparison of power consumption for nanolubricants at different outdoor temperatures and concentrations.

refrigerant effect results. Fig. 10 depicts the compressor work trend of different outdoor temperatures for SiO_2/PVE and TiO_2/PVE at different concentrations.

The compressor work for all tested samples showed an increasing trend with the increment of outdoor temperature. Lower compressor work is better for the VCR cycle because it brings the meaning of less energy used to produce the same amount of cooling effect. The nanolubricants show lower compressor work than pure PVE lubricants. Interestingly, the compressor work at 35 °C showed a maximum decrement compared to at other temperatures. The compressor work increased linearly with the increment of outdoor temperatures except for 35 °C. The linear trend happened at both types of nanolubricants at all concentrations. The SiO_2/PVE at 0.005 % concentration showed the most excellent decrement at all temperatures except for 31 °C. The addition of nanoparticles in compressor lubricant contributed to a better tribological effect on the compressor. Nanoparticles dispersed in the PVE lubricant form a protective lubrication layer on contact surfaces, reducing friction and mechanical losses during compression. The compression process with nanolubricants became smoother than that of PVE lubricant. This situation made the compressor compress more refrigerant within the same period of operation, and the refrigerant mass flow rate increased.

The results of mass flow rate and compressor work for nanolubricants above had demonstrated the reason why the refrigerant effects of nanolubricants were lower than that for the pure lubricant. Compared to the compressor used by Sharif, Azmi [44], the current study used a different type of compressor. The RAC system in the current study used a rotary type compressor driven by electrical energy, while the AAC system used by Sharif, Azmi [44] was a vane type compressor driven by an engine through a belt. The nature of the operating condition of the two systems was different, and this made the results different. Nevertheless, the nanolubricants in the current study showed its capability to change the performance parameter of RAC towards improvement. The following subsection discusses the results of the same parameters for hybrid nanolubricants.

3.6. Nanoparticle effect on RAC performance

Fig. 11 presents the results for cooling capacity of PVE lubricant with the nanolubricants for specified outdoor temperatures of 31 until 39 °C. The result in this figure shows that the cooling capacity for pure PVE fell between 1.6 and 3.6 kW. Meanwhile, the cooling capacity for nanolubricants shows result value between 1.6 and 4.5 kW. Most nanolubricants at different concentrations show higher cooling capacity value compared to that of pure PVE. The cooling capacity results in this figure seemed to follow the trend of the mass flow rate presented previously (Fig. 9), where the mass flow rate decreased with the increment of outdoor temperatures. An overview of the cooling capacity results showed that all nanolubricants had a higher cooling capacity compared to that of pure PVE except for SiO_2/PVE at 0.003 % concentration. The significant increment happened at 31 °C while increment towards higher outdoor temperatures, i.e., 37 and 39 °C, seemed to be smaller. There was no significant difference in cooling capacity increment in SiO_2/PVE and TiO_2/PVE nanolubricants. The trend of cooling capacity was dominated by the trend of mass flow rate because the mass flow rate value was relatively small, i.e., 0.007–0.014 kg/s, compared to that of the refrigerant effect, i.e., between 230 and 250 kJ/kg. Even though the effectiveness of the evaporator dropped by the reduction of refrigerant effect for nanolubricants, the increment of mass flow rate had encountered reduction by absorbing more heat from the indoor areas. The heat transfer effects produced by the mass flow rate increment were much higher than the refrigerant effect reduction. This made the cooling capacity for nanolubricants increase

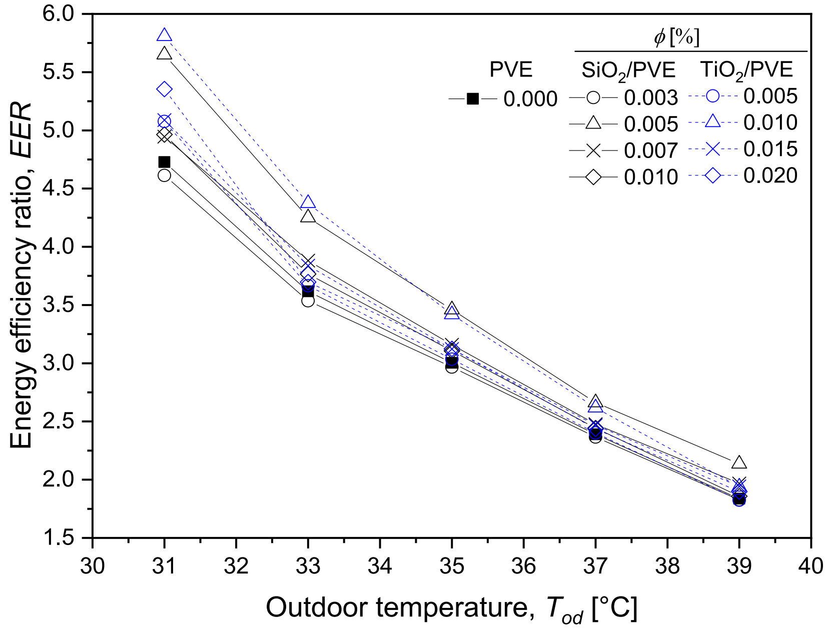

Fig. 13. Comparison of EER for nanolubricants at different outdoor temperatures and concentrations.

significantly.

Moving to the other parameter measured for RAC system performance evaluation is the power consumption. The power consumption in the current study was measured at two different points for comparison purposes. The first point was the total power consumption (Psys) and the second point was the power to the compressor (Pcomp). Psys was the electrical power input to the RAC that includes the power to the compressor, the power to the indoor blower and condenser fan, and the power to all controls and safety devices. Meanwhile, Pcomp was only counted the power supplied to the compressor. Results for both power consumptions are shown in Fig. 12.

Since the other operating condition of the experiment was set to be constant, the variables that influenced the performance of RAC were only the outdoor temperature and the concentration of nanoparticles. The effect of the changes in power consumption was not influenced by other parameters than these two. The Psys and Pcomp increased by the increment of outdoor temperature. Most nanolubricants reduced the Psys and Pcomp in comparison to their respective baseline. On average, there was a difference of 0.08 kW in Psys compared to Pcomp. This difference represents the amount of power Psys and Pcomp used by other devices than the compressor. In comparison of power consume by pure PVE with nanolubricants, the result in this figure shown that there was no significant difference. The results only shows that the second studied concentrations for both nanolubricants (0.005 % for SiO_2/PVE and 0.010 % for TiO_2/PVE) had the lowest power consumption compared to that of PVE lubricant. The discussion on the relationship between cooling capacity and power consumption for nanolubricants was presented in the subsection after the presentation of cooling capacity and power consumption results for hybrid nanolubricants.

The final parameter used to evaluate the performance of the RAC system was the EER. Fig. 13 presents the EER for nanolubricants at different outdoor temperatures and concentrations. EER is the ratio between the cooling capacity and the total power consumption of RAC systems. The EER results in Fig. 13 shows that it decreases with the increase in outdoor temperatures. The SiO_2/PVE at 0.003 % concentration showed a lower EER value compared to that of pure PVE at all temperatures. In contrast, other nanolubricants showed increment in EER throughout all points of outdoor temperatures. The highest increment appeared at 31 °C for the TiO_2/PVE 0.010 % concentration. The trend also showed that the EER was most influenced by cooling capacity instead of by power consumption due to its trend was similar to the trend of cooling capacity. The trends of cooling capacity and EER in the current study were verified by previous findings from the literature. Wang, Wu [49] stated that the cooling capacity and EER decreased with the increment of temperature. Moreover, the addition of nanoparticles in compressor lubricant increases the EER of the system.

The effect of nanoparticle concentration on the performance of the VCR cycle as well as the RAC system is best presented in relative percentages. Relative percentage gave us information about the enhancement of COP and EER for nanolubricants relative to the same parameter values for pure PVE lubricant. Fig. 14 (a) shows the comparison of COP changes for nanolubricants relative to pure PVE. While Fig. 14 (b) shows the comparison of EER changes for nanolubricants relative to pure PVE.

The COP showed increment for all nanolubricants at all measured outdoor temperatures. Overall trend of relative COP for both nanolubricants shows that the COP increment started with low increment at the first studied concentration. The highest increment appeared at the second concentration for each type of nanolubricants. The following concentration showed lower increment than the second but higher than the first concentration. This decrement trend was continued for the final concentration. SiO_2/PVE nanolubricants showed maximum COP increment up to 23 % leaving the TiO_2/PVE nanolubricants at 17 %. This maximum enhancement

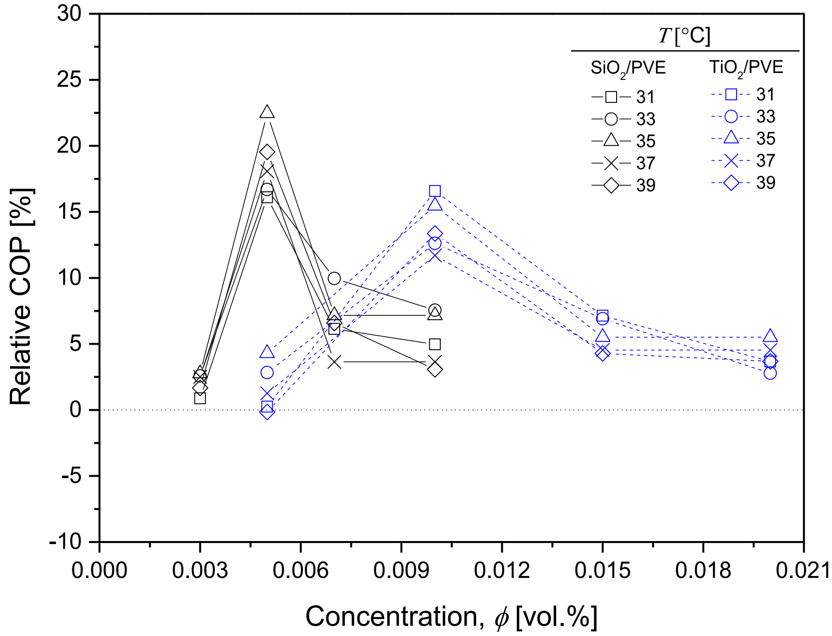

(a) Relative COP

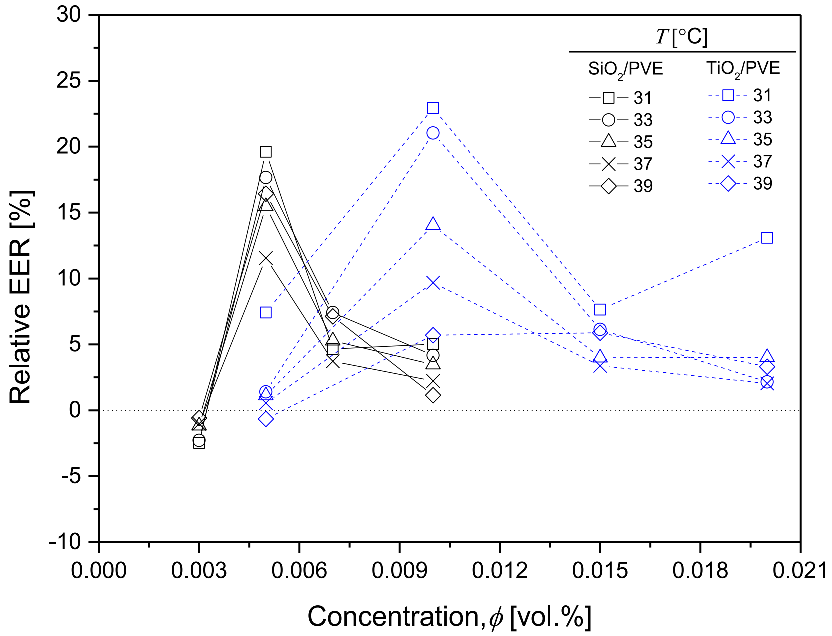

(b) Relative EER

Fig. 14. Relative (a) COP and (b) EER comparison at different nanoparticle concentration.

happened at different concentration and outdoor temperatures: 0.005 % at 35 °C and 0.010 % at 31 °C for SiO_2/PVE and TiO_2/PVE nanolubricants, respectively. The addition of nanoparticle concentration slowly increased the COP value until the COP reached the maximum value. Further increment of nanoparticles that exceeded this limit did not contribute to further increment of relative COP but further reduced the relative COP.

Moving to Fig. 14 (b) is the relative EER results for nanolubricants. On one hand, the SiO_2/PVE nanolubricants showed maximum EER increment up to 20 % at 0.005 % concentration. On the other hand, the TiO_2/PVE nanolubricants showed maximum EER increment up to 22 % at 0.010 % concentration. The relative EER results showed the same trend as relative COP where the EER increased when volume concentration increases. When the concentration reached the threshold value, the EER started to decrease when the volume concentration was further increases. Interesting result shown in EER was the maximum EER enhancement happened at 31 °C for both nanolubricants. Although nanolubricants offer measurable performance improvement, their application may present potential disadvantages if not carefully controlled. At higher nanoparticle concentrations, agglomeration and increased lubricant viscosity may occur, which can restrict refrigerant flow, reduce heat transfer effectiveness, and increase mechanical stress on compressor components. In addition, long term operation may raise concerns related to particle deposition, wear, and possible material interaction. In the present study, these effects were minimized by using very low nanoparticle concentrations and by verifying short term stability prior to system testing. Long term durability and material compatibility remain important topics for future investigation.

From Fig. 14 and other results in this section discussed previously, a conclusion can be made that SiO_2/PVE nanolubricants perform better than that of TiO_2/PVE nanolubricants. SiO_2/PVE nanolubricants performed better in COP which represented better effect on VCR cycle performance when the SiO_2 nanoparticle was dispersed in PVE lubricant. This performance increment was contributed by lower compressor works performed by this nanolubricants compared to that of the pure PVE lubricant. Better performance in tribology was the reason of lower compressor works. As depicted in previous study, the COP for SiO_2/PVE nanolubricants at volume concentration of 0.003 and 0005 % was lower than 0.10 compared to that of TiO_2/PVE nanolubricants which was 0.12 [50]. Additionally, the studied volume concentration range for SiO_2/PVE nanolubricants was lower than that of the TiO_2/PVE nanolubricants. This is another reason to justify that SiO_2/PVE nanolubricants performed better than TiO_2/PVE nanolubricants.

4. Conclusions

This study evaluated the effect of SiO_2 and TiO_2 nanoparticle additives dispersed in polyvinyl ether lubricant on the performance of a residential air conditioning system operating with R32 refrigerant. The objective was to assess whether nanolubricant modification can enhance system performance under realistic operating conditions without hardware modification.

Experimental results show that replacing the original refrigerant with R32 reduced the required refrigerant charge from 540 g to 350 g while maintaining stable operation. The addition of nanoparticles reduced compressor work and increased refrigerant mass flow rate, resulting in higher cooling capacity and improved energy efficiency. Maximum performance enhancement was achieved at low nanoparticle concentrations. SiO_2 at 0.005 vol% increased the coefficient of performance by up to 23 percent and the energy efficiency ratio by up to 20 percent. TiO_2 at 0.010 vol% produced a COP improvement of up to 17 percent and an EER improvement of up to 22 percent. At concentrations above these thresholds, further performance gains were not observed, indicating an optimal additive range.

The results confirm that PVE based nanolubricants are compatible with R32 and can significantly improve residential air conditioning performance using only milligram scale additive quantities. These findings demonstrate that nanolubricant application offers a practical pathway for improving energy efficiency in low GWP air conditioning systems without system redesign. Further analysis on the optimum nanoparticle concentration that provides the best performance on RAC is recommended. The study on PVE nanolubricants miscibility and the physical impact of nanoparticles on the electrical motor in the compressor are also possible for future work.

CRediT authorship contribution statement

M.F. Ismail: Writing – original draft, Project administration. **M.Z. Sharif:** Writing – review & editing, Data curation, Conceptualization. **M.M. Sulhan:** Resources, Formal analysis.

Declaration of competing interest

The authors declare that they have no known competing financial interests or personal relationships that could have appeared to influence the work reported in this paper.

Acknowledgment

The authors are grateful to the Universiti Teknikal Malaysia Melaka (www.utem.edu.my) for laboratory facilities and financial supports given under International grant ASHRAE A00059. Also, the authors would like to also thank the research teams from Green and Efficient Energy Technologies who have provided professional insights and expertise that greatly assisted the present research work.

Abbreviations

CFC	Chlorofluorocarbon
COF	Coefficient of friction
COP	Coefficient of performance
EER	Energy efficiency ratio
GWP	Global warming potential
HCFC	Hydrochlorofluorocarbon

HFC	Hydrofluorocarbon
HRTEM	High-resolution transmission electron microscope
POE	Polyol ester
PVE	Polyvinyl ether
RSE	Relative standard error
RAC	Residential air conditioning
TCR	Thermal control room
TEM	Transmission Electron Microscopy
TEWI	Total equivalent warming impact
VCR	Vapor Compression Refrigeration

Nomenclature

W_{in}	Compressor work
P_{comp}	Compressor power consumption
$\dot{q}_c$	Cooling capacity
d_p	Diameter of nanoparticle
h	Enthalpy
$\dot{m}$	Mass flowrate
m_l	Mass of PVE lubricant
m_n	Mass of nanoparticle
M	Molecular mass
Tod	Outdoor temperature
P	Pressure
m_R	Refrigerant charge
q_{in}	Refrigerant effect
c_p	Specific heat
T	Temperature
P_{sys}	Total power consumption

Greek symbols

ρ	Density
ρ_n	Density of nanoparticle
ρ_l	Density of PVE lubricant
σ	Standard deviation
$\varnothing$	Volume concentration

Data availability

The authors confirm that the data supporting the findings of this study are available within the article.

References

[1] Exxon-Mobil, Outlook for energy: a perspective to 2040, in: Outlook for Energy. 2019, Exxon Mobil Corporation, Texas, USA, 2019.
[2] T.M.I. Mahlia, R. Saidur, A review on test procedure, energy efficiency standards and energy labels for room air conditioners and refrigerator–freezers, Renew. Sustain. Energy Rev. 14 (7) (2010) 1888–1900.
[3] JRAIA, World air conditioner demand by region, in: World Air Conditioner Demand by Region, The Japan Refrigeration and Air Conditioning Industries Association, 2019.
[4] R. Ciconkov, Refrigerants: there is still no vision for sustainable solutions, Int. J. Refrig. 86 (2018) 441–448.
[5] UNEP, The kigali amendment to the Montreal protocol : HFC phase-down, in: OzonAction, UN Environment (UNEP), Paris, France, 2016, pp. 1–7.
[6] S. Taira, T. Haikawa, T. Minamida, Evaluation of performance of heat pump using R32 and HFO-Mixed refrigerant by refrigeration cycle simulation and loss analysis, in: International Refrigeration and Air Conditioning Conference, Purdue, 2016.
[7] R. Yajima, et al., R32 as a solution for energy conservation and low emission, in: International Refrigeration and Air Conditioning Conference, 2000.
[8] X.H. Wu, Z. Yang, Y.Y. Duan, Evaporation of R32/R1234yf mixture nanodroplets on a smooth substrate: molecular dynamics simulation, Chem. Phys. Lett. (2019) 733.
[9] D.F. Marcucci Pico, et al., Experimental study on thermal and tribological performance of diamond nanolubricants applied to a refrigeration system using R32, Int. J. Heat Mass Tran. 152 (2020) 119493.
[10] I. Tlili, S.Z. Khan, A. Aljabri, Improvement in thermal phenomenon due to bioconvective transport of third-grade nanomaterial with variable viscosity and convective boundary constraints: sustainable energy developments, Case Stud. Therm. Eng. 73 (2025) 106483.
[11] A.M. Alkalibi, Y.H. Alahmadi, I. Tlili, Performance analysis of an extended-surface double-pipe heat exchanger for heat recovery from hot exhaust gas using water and nanofluids, Results Eng. 27 (2025) 106140.
[12] A.M. Alklaibi, S.e.A. Musmar, I. Tlili, Numerical simulation of double-pipe helical coil heat exchangers: influence of geometry and nanofluid on heat transfer enhancement, Results Eng. 28 (2025) 107053.

[13] I. Tlili, Computational analysis for thermo-diffusion applications of concentrated tri-hybrid nanoparticles with nonlinear radiated effects: the non-classical thermal model, Applied Mathematics in Science and Engineering 33 (1) (2025) 2511753.
[14] I. Tlili, Neural network analysis for unsteady flow of viscoelastic nanofluid with slip effects, Pramana 99 (3) (2025) 126.
[15] H. Masuda, et al., *Alteration of thermal conductivity and viscosity of liquid by dispersing ultra-fine particles. Dispersion of Al_2O_3, SiO_2 and TiO_2 ultra-fine particles*, Netsu Bussei 7 (4) (1993) 227–233.
[16] S.U.S. Choi, J.A. Eastman, Enhancing thermal conductivity of fluids with nanoparticles, in: ASME International Mechanical Engineering Congress & Exposition, Argonne National Lab., IL: United States, 1995.
[17] L. Yang, et al., A review of heating/cooling processes using nanomaterials suspended in refrigerants and lubricants, Int. J. Heat Mass Tran. 153 (2020) 119611.
[18] M.R.M. Nawi, et al., *The characterization and thermo-physical property investigations of SiO_2/HFE7000 nanorefrigerants*, Int. J. Refrig. 88 (2018) 275–283.
[19] O.A. Alawi, N.A.C. Sidik, H.A. Mohammed, A comprehensive review of fundamentals, preparation and applications of nanorefrigerants, Int. Commun. Heat Mass Tran. 54 (2014) 81–95.
[20] T.A. Moreira, D.C. Moreira, G. Ribatski, Nanofluids for heat transfer applications: a review, J. Braz. Soc. Mech. Sci. Eng. 40 (6) (2018) 1–29.
[21] D. Jige, et al., Two-phase flow characteristics of R32 in horizontal multiport minichannels: flow visualization and development of flow regime map, International Journal of Refrigeration-Revue Internationale Du Froid 95 (2018) 156–164.
[22] G. Lillo, et al., Flow boiling of R32 in a horizontal stainless steel tube with 6.00 mm ID. Experiments, assessment of correlations and comparison with refrigerant R410A, International Journal of Refrigeration-Revue Internationale Du Froid 97 (2019) 143–156.
[23] D.V.R.R.C. Venugopal, D.R. Reddy, A review on performance of vapour compression refrigeration system using nano additive refrigerants, AASCIT Journal of Nanoscience 4 (1) (2018) 14–18.
[24] B. Jalili, H. Ghafoori, P. Jalili, Investigation of carbon nano-tube (CNT) particles effect on the performance of a refrigeration cycle, International Journal of Material Science Innovations 2 (1) (2014) 8–17.
[25] T. Jia, et al., Solubilities of difluoromethane (R32) in polyol ester, polyvinylether, and polyalkylene glycol base oils at temperatures from 273 K to 351 K, Int. J. Refrig. 111 (2020) 63–70.
[26] Idemitsu Kosan, C.L. *Characteristics of Daphne Hermetic Oil*, Daphne hermetic oil FV series 2020 [cited 2020 1/1/2020]; Available from: www.idemitsu.com/business/lube/pve/daphne.html.
[27] M. Kaneko, et al., Determination of properties of PVE lubricants with HFC refrigerants, ASHRAE Transactions 105 (1999) 1000.
[28] M. Kaneko, J.-i. Yagi, S. Tominaga, The evaluation of PVE (poly vinyl ether) as a lubricant for air conditioning system converted from HCFC22 to either HFC410A or HFC407C, in: International Refrigeration and Air Conditioning Conference, Purdue e-Pubs: Purdue, 2004, pp. 1–7.
[29] T. Matsumoto, M. Kaneko, M. Tamano, Properties of polyvinylether (PVE) as a lubricant for air conditioning systems with HFC refrigerants? Data update?, in: International Refrigeration and Air Conditioning Conference Purdue e-Pubs: Purdue, 2010, pp. 1–8.
[30] M. Motozawa, N. Makida, M. Fukuta, Experimental study on physical properties of CuO - PVE nano-oil and its mixture with refrigerant, in: International Compressor Engineering Conference, Purdue, 2018.
[31] A. Senthilkumar, A. Anderson, R. Praveen, Prospective of nanolubricants and nano refrigerants on energy saving in vapour compression refrigeration system – a review, Mater. Today Proc. 33 (2020) 886–889.
[32] M.F. Nabil, et al., *An experimental study on the thermal conductivity and dynamic viscosity of TiO_2-SiO_2 nanofluids in water: ethylene glycol mixture*, Int. Commun. Heat Mass Tran. 86 (2017) 181–189.
[33] R. Krishna Sabareesh, et al., Application of TiO_2 nanoparticles as a lubricant-additive for vapor compression refrigeration systems – an experimental investigation, Int. J. Refrig. 35 (7) (2012) 1989–1996.
[34] G. Jatinder, et al., *Performance of a domestic refrigerator using selected hydrocarbon working fluids and TiO_2–MO nanolubricant*, Appl. Therm. Eng. (2019) 160.
[35] O.S. Ohunakin, et al., Performance of a hydrocarbon driven domestic refrigerator based on varying concentration of SiO_2 nano-lubricant, Int. J. Refrig. 94 (2018) 59–70.
[36] N.N.M. Zawawi, et al., Thermo-physical properties of metal oxides composite nanolubricants, J. Mech. Eng. 5 (2018) 28–38.
[37] M.F. Ismail, et al., *Extensive stability assessment of TiO_2/Polyvinyl ether nanolubricant with physical homogenization*, Lubricants 11 (2) (2023).
[38] M.F. Ismail, et al., *Stability assessment of polyvinyl-ether-based TiO_2, SiO_2, and their hybrid nanolubricants*, Lubricants 11 (1) (2023).
[39] N. Sezer, M.A. Atieh, M. Koc, A comprehensive review on synthesis, stability, thermophysical properties, and characterization of nanofluids, Powder Technol. 344 (2019) 404–431.
[40] A.A.M. Redhwan, et al., Development of nanolubricant automotive air conditioning (AAC) test rig, in: MATEC Web of Conferences, vol. 90, 2017.
[41] M.Y. Taib, A.A. Aziz, A.B.S. Alias, Performance analysis of a domestic refrigerator, in: National Conference in Mechanical Engineering Research and Postgraduate Students, 2010, pp. 582–591. Kuantan, Pahang, Malaysia.
[42] M.Z. Sharif, et al., Comparative air conditioning performance using SiO_2 and Al_2O_3 nanolubricants operating with Hydrofluoroolefin-1234yf refrigerant, Appl. Therm. Eng. 205 (2022).
[43] A.A.M. Redhwan, et al., *Performance improvement in mobile air conditioning system using Al_2O_3/PAG nanolubricant*, J. Therm. Anal. Calorim. 135 (2) (2019) 1299–1310.
[44] M.Z. Sharif, et al., *Performance analysis of SiO_2/PAG nanolubricant in automotive air conditioning system*, Int. J. Refrig. 75 (2017) 204–216.
[45] A.H. Hamisa, et al., *The stability of TiO_2/POE nanolubricant for automotive air-conditioning system of hybrid electric vehicles*, in: IOP Conference Series: Materials Science and Engineering, Institute of Physics Publishing, 2020 012050.
[46] A. Ghadimi, R. Saidur, H.S.C. Metselaar, A review of nanofluid stability properties and characterization in stationary conditions, Int. J. Heat Mass Tran. 54 (2011) 4051–4068.
[47] M.F. Ismail, et al., Thermal and tribological properties enhancement of PVE lubricant modified with SiO_2 and TiO_2 nanoparticles additive, Nanomaterials 13 (1) (2023) 42.
[48] R. Harichandran, et al., Effect of h-BN solid nanolubricant on the performance of R134a–polyolester oil-based vapour compression refrigeration system, J. Braz. Soc. Mech. Sci. Eng. 41 (3) (2019).
[49] R. Wang, Q. Wu, Y. Wu, Use of nanoparticles to make mineral oil lubricants feasible for use in a residential air conditioner employing hydro-fluorocarbons refrigerants, Energy Build. 42 (11) (2010) 2111–2117.
[50] M.F. Ismail, et al., Thermal and tribological properties enhancement of PVE lubricant modified with SiO2 and TiO2 nanoparticles additive, Nanomaterials 13 (1) (2023).
[51] S.X. Xu, X.S. Fan, G.Y. Ma, Experimental investigation on heating performance of gas-injected scroll compressor using R32, R1234yf and their 20wt%/80wt% mixture under low ambient temperature, International Journal of Refrigeration-Revue Internationale Du Froid 75 (2017) 286–292.
[52] G.L. Hongwu International, Anatase nano TiO_2 titanium dioxide powders [cited 2021 25/9/2021]; Available from: www.hwnanomaterial.com/anatase-nano-tio2-titanium-dioxide-powders_p49.html, 2021.
[53] S.A.T.C.L. Beijing Deke Daojin, Nano silica [cited 2021 25/9/2021]; Available from: www.dknano.com/Ecplb.asp?Fid=1177&ClassId=1190&NewsId=2993, 2021.
[54] International Organization for Standardization, I, ISO 5151-2010 Non-ducted Air Conditioners and Heat Pumps — Testing and Rating for Performance, International Organization for Standardization (ISO), Switzerland, 2010.